Mater. Res. Soc. Symp. Proc. Vol. 1818 © 2016 Materials Research Society
DOI: 10.1557/opl.2016.81

Dislocation study of ARMCO iron processed by ECAP

Jairo Alberto Muñoz[1,a], Oscar Fabián Higuera[1, 2, b] , José María Cabrera[1, 3, c]

[1]Department of Materials Science and Metallurgical Engineering ETSEIB, Universidad Politécnica de Catalunya, Av Diagonal 647, 08028 Barcelona, Spain.

[2]Faculty of Mechanical Engineering, Universidad del Atlántico, Colombia

[3]Fundació CTM Centre Tecnológic, Pl. de la Ciencia 2, 08243, Manresa, Spain.

[a]jairo.alberto.munoz@upc.edu, [b]osfahico@gmail.com, [c]jose.maria.cabrera@upc.edu

ABSTRACT

The aim of this work was to study the deformation behavior of an Armco iron after severe plastic deformation by equal channel angular pressing (ECAP). Particular attention was paid to predict the dislocation density by different approaches like the model proposed by Bergström. Experimental measures of dislocation density by different techniques are used in the discussion. Cylindrical samples of ARMCO iron (8mm of diameter, 60mm of length) were subjected to ECAP deformation using a die with an intersecting channel of Φ=90º and outer arc of curvature of ψ= 37° die. Samples were deformed for up to 16 ECAP passes following route Bc. The mechanical properties of the material were measured after each pass by tensile tests. The original grain size of the annealed iron (70 μm) was drastically reduced after ECAP reaching grain sizes close to 300nm after 16 passes.

INTRODUCTION

During large plastic deformation of metals and alloys, the original grain structure develops a microstructure on a much smaller scale. Ultra fine grain (UFG) materials are quite attractive due to the ultrahigh strength they can attain, which is more than twice that of their coarse grained counterparts. The movement of dislocations constitutes the fundamental basis for understanding the plastic behavior of crystalline materials [1], and this fact becomes specially important in analyzing the plastic behavior of UFG materials, where controversial results can be found in the literature concerning the role played by dislocations and their limited motion capability. Under this point of view scarce studies can be found in the literature concerning the dislocation density evolution during a severe plastic deformation process. Length scales associated with dislocation structures range from grain-size features (typically 0.1–10 mm) down to perhaps tens of atoms (1–10 nm). Because of this large range, a good characterization normally requires a combination of techniques [2]. Dislocation density (measured as number of lines per unit area, or length per unit volume) in thin foils can be

measured directly using TEM. TEM measurements are experimentally challenging (problems include sample preparation, and finding imaging conditions for all dislocations), and thin films may not be representative of bulk material . X-ray line profile analysis is also a versatile technique that can be used for determining dislocation densities in bulk samples [2].

EXPERIMENTAL PROCEDURE

A commercial ARMCO iron (Fe-0.01%C-0.01%Si-0.059%Mn-<0.01%P-<0.010%S-0.02%Cr-<0.005%Mo-0.038%Ni-0.013%Al (in wt%)) was received in the form of rods of 8mm in diameter. The rods were divided into short billets having lengths of ~60mm, and these billets were subjected to severe plastic deformation by Equal Channel Angular Pressing (ECAP) at room temperature. Samples were severely deformed up to a maximum equivalent strain of 16 (i.e., 1, 2, 3, 4, 5, 6, 7, 8 and 16 ECAP passes) following route Bc. An ECAP die with an inner angle of $\Phi = 90^{o}$ and an outer angle of $\psi = 37^{o}$ was used (see Figure 1). Tensile samples were machined form the deformed samples, and tested at room temperature. These tests were carried out at a constant crosshead speed of $3.3x10^{-3}$ mm/s until failure. The microstructure of the samples was characterized by Electron Backscattered Diffraction (EBSD), Transmission Electron Microscopy (TEM) and X-ray line profile analysis (XRLPA). EBSD specimens were cut from the centre of the ECAP samples and mechanically polished from 2500 grit SiC paper until 0.02μm colloidal silica suspension, following standard metallographic procedures. TEM samples were also cut from the centre of the ECAPed samples and mechanically polished until a thickness of ~80μm. Then they were electropolished at room temperature using 6% perchloric acid ($HClO_4$) +94% glacial acetic acid (CH_3COOH) for 2-3 minutes. In the case of the XRLPA study, samples were cut from the longitudinal section of deformed specimens. A PANalytical X'Pert PRO MPD diffractometer equipped with a dual goniometer of Cu-Kα (λ=1.5406μm) was employed.

RESULTS AND DISCUSSION

The microstructures before and after ECAP passes are shown in Figure **2**. The as-received material consists mainly of equiaxed grains. The initial microstructure is mainly formed by High Angle Grain Boundaries (HAGB) due to the annealed state. The average grain size calculated by EBSD was ~72μm. After the first pass the microstructure became reoriented and shear strained (see Figure **2**) with an average grain size of 1.89μm, It must be noted that the microstructure is heterogeneous, formed by large elongated grains and very fine equiaxed ones, with a noticeable amount of Low Angle Grain Boundaries (LAGB). After 4 and 8

https://doi.org/10.1557/opl.2016.81

passes the microstructure turned out smaller and equiaxed. An increment in HAGB with respect to the material with one pass was noticed. Grain sizes of 435nm and 365nm were attained respectively. This observation can be explained by the generation of geometrically necessary boundaries which in turns subdivide the coarse grains into cell blocks [3]. Accordingly HAGB continuously increase after the first ECAP pass (see Figure 3). Finally after 16 ECAP passes the fraction of HAGB is higher than the one of LAGB since the microstructure is almost totally formed by equiaxed grains with an average grain size of 275nm. Thus the microstructure has been regenerated with a smaller grain size as a result of the new arrangement of dislocations [4].

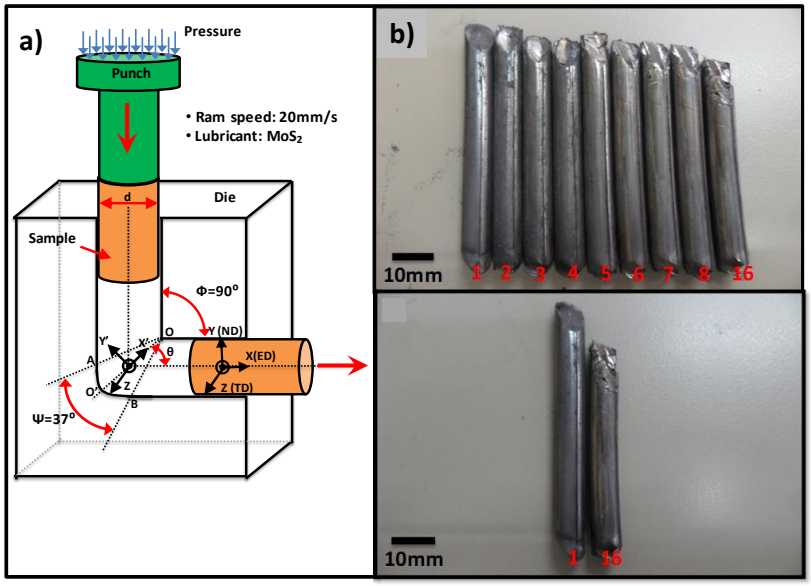

Figure 1. a) ECAP die configuration and b) samples processed by ECAP.

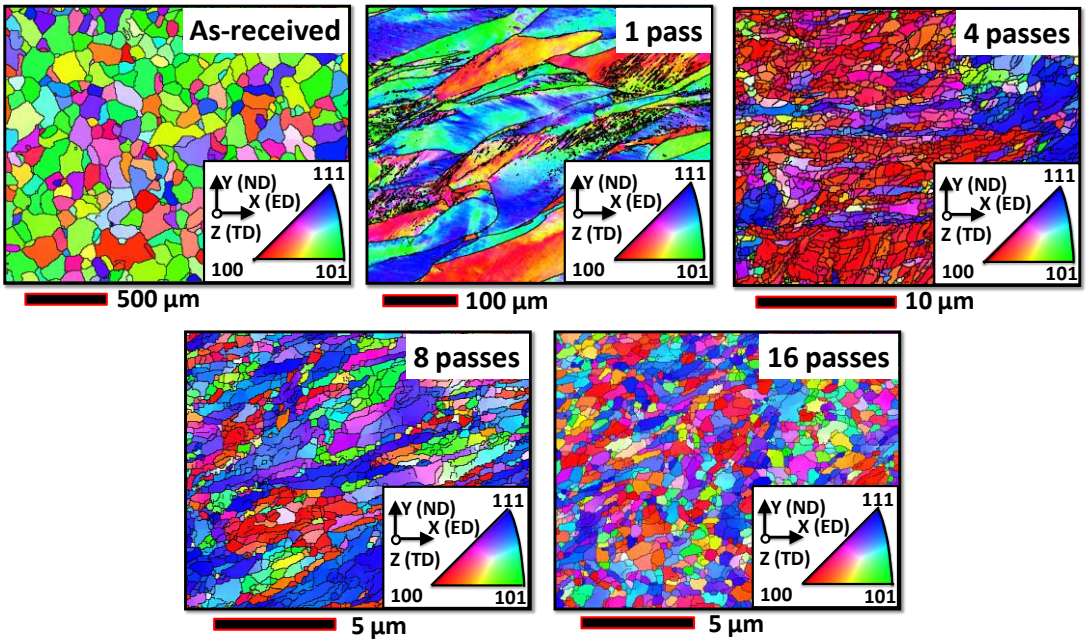

Figure 2. Microstructures of ARMCO-Fe before and after ECAP at different number of passes

A comparison of the most important fractions of Coincident Site Lattice (CSL) for the material before and after ECAP is also shown in Figure 3. It is clearly observed that all the CSL fractions are reduced after ECAP in comparison with the as-received material. However with the increase in the deformation the percentages of special boundaries increase until 16 passes, where the highest fraction of total CSL is obtained among the different ECAP passes.

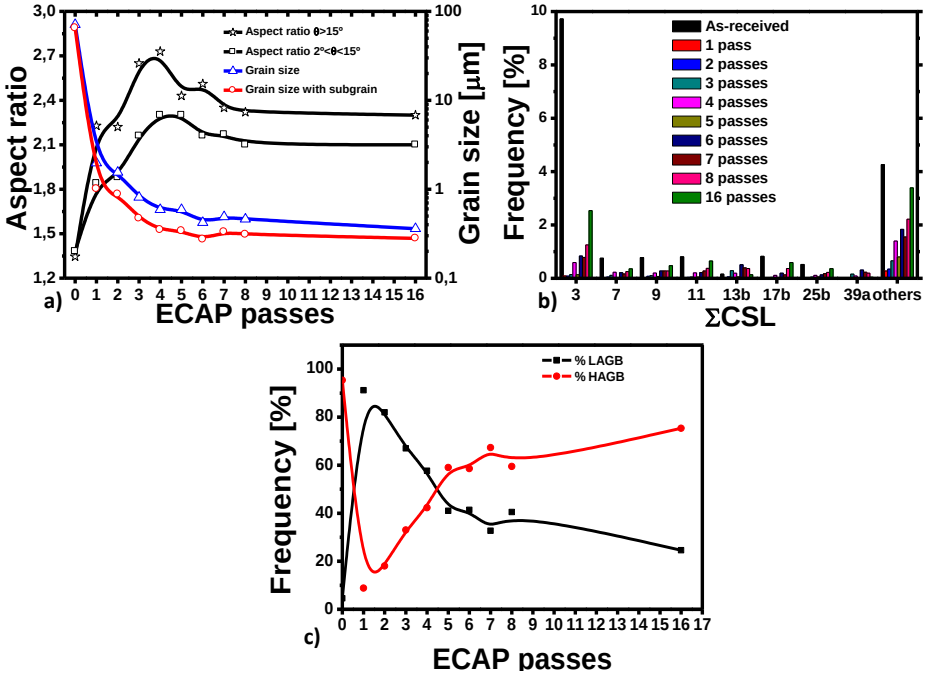

Figure 3. Microstructural properties a) grain size and aspect ratio, b) CSL percentages and c) LAGB and HAGB evolution.

The effect of number of ECAP pass on the mechanical properties at room temperature, plotted in the form of engineering stress-strain and true stress-strain curves, is shown in Figure 4. Firstly it is observed that the annealed sample showed a larger uniform deformation (~22%) than the corresponding material deformed by ECAP (less than 4% for all the passes). In general, the engineering stress-strain curves of the processed material showed the maximum strength at the early stage of deformation, followed by a region of plastic instability (necking appearance) until failure. The yield stress σ_y, ultimate tensile strength σ_{UTS} and the uniform deformation for the annealed material are 204MPa, 277MPa and 22.49% respectively. After four ECAP passes, a strong increase in strength (σ_y = 645MPa, σ_{UTS} = 700MPa) with a significant decrease in ductility (uniform deformation of 1.27%) was observed. Similar values of yield stress and strength were reported by Gang et al [5] in a pure iron with 99.86% Fe processed up to 4 ECAP passes. Nevertheless after the 6th pass there is an increment in the uniform elongation as shown in Figure **4**b. It is important to notice that material with 16 passes present an increment of ~3 times in strength with respect to the annealed material

reaching 904MPa which is quite similar to the values reported for low carbon steels processed by ECAP [6,7].

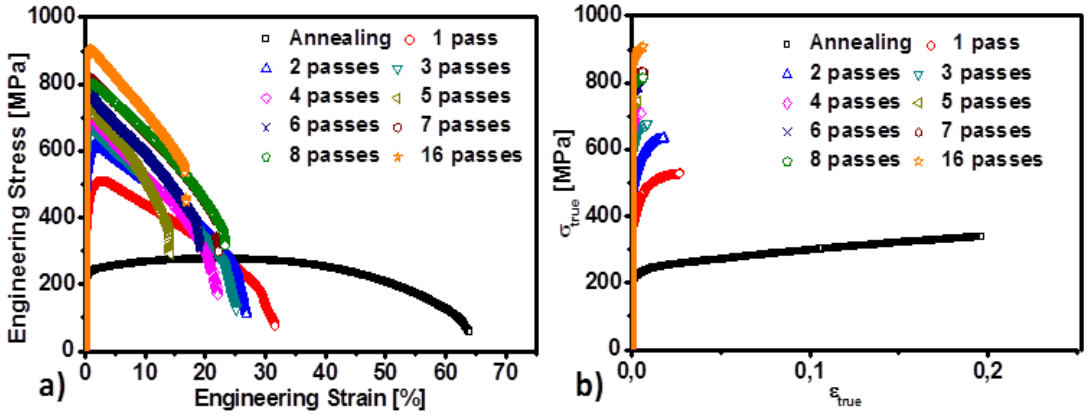

Figure 4. Tensile curves. (a) Engineering stress-strain curves; (b) True stress-strain curves before necking.

To calculate the dislocation density before and after ECAP for the different number of passes several techniques and approaches were used, namely, 1) TEM by the line intercept method [8, 9], 2) XRDLPA using Rietveld refinements with the MAUD software [10]. 3) Fitting the true stress-strain curve to the theoretical model proposed by Bergström [1].

The first method was proposed by U. Martin et al [8] and it was here applied following the procedure described in [9]. Accordingly, the dislocation density calculated for different numbers of passes is shown in Figure 7 (green line). These values are a little bit different in comparison with those reported by Ivanov et al [11] (Figure 7 blue line). This could be attributed to the different routes employed in these two studies (Route Bc in the present study and Route A for Ivanov et al [11]) which leads to differences in the microstructures produced by ECAP because of different gliding systems are activated [12].

The second method consist in analyzing the XRD patterns of the samples as shown in Figure **5**a depicts recorded before and after ECAP. It contains the (110), (200), (211), (200) and (310) reflections of the Fe phase. With increasing number of passes, a broadening of the diffraction peaks is notorious. As well the continuous decrease in the peak heights originated from a reduction in the crystalline size, faulting and microstrains within the diffracting domains, can also be observed in Figure **5**b and c. In addition, the examination of diffraction patterns during ECAP shows that peaks are shifted to low θ values. This can be explained by i) the creation of stacking faults by intensive deformation and ii) the change of the lattice parameter during ECAP.

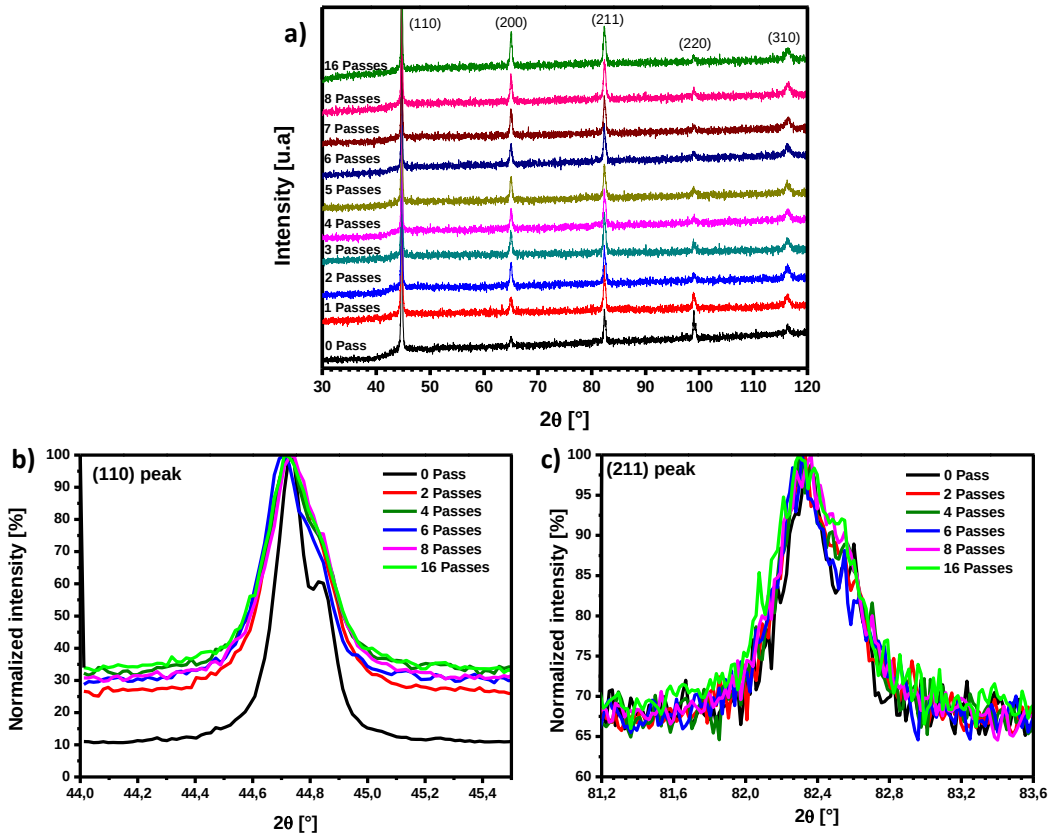

Figure 5. a) X-ray diffraction patterns before and after ECAP. Bragg reflections as a function of the number of passes for b) (110) peak and c) (211) peak.

The evolution of the crystallite sizes and the lattice strains as a function of the number of passes are given in Figure **6**. A strong decrease of the crystal size D is observed since the first pass accompanied by a substantial increase of the lattice strain ε. This can be explained in terms of the high amount of deformation introduced. A value of 136 nm is attained after 16 ECAP passes. On the contrary, the lattice strain increases up to 0.86% after 16 ECAP passes. This behavior can be caused only by plastic deformation which will raise the lattice strain because of the increase of the defect density as well as dislocations grain boundaries and lattice defects, in the initially relatively defect-free material.

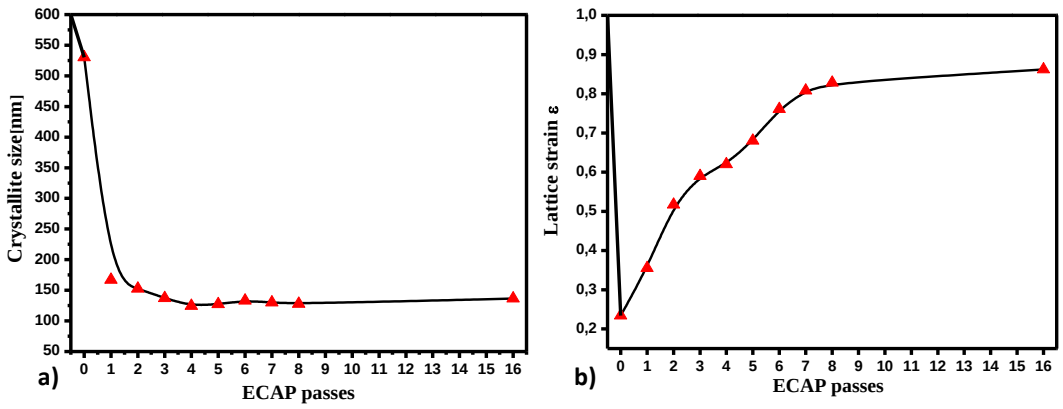

Figure 6. Evolutions of the a) crystallite sizes and b) the lattice strain as a function of the number of passes.

https://doi.org/10.1557/opl.2016.81

The dislocation density ρ, can be expressed in terms of the crystallite size D and the mean lattice strains $\langle \varepsilon^2 \rangle^{1/2}$ as [13, 14]:

$$\rho = 2\sqrt{3}\frac{\langle \varepsilon^2 \rangle^{1/2}}{\langle D \rangle b} \quad (1)$$

It is clearly seen in Figure **7** (red line) that ρ increases from about 2.96×10^{14} to 9.01×10^{14} m^{-2} with the number of ECAP passes increasing from 1 to 8 and then remained unchanged at a steady-state value of about $8.80 \times 10^{14}\,m^{-2}$.

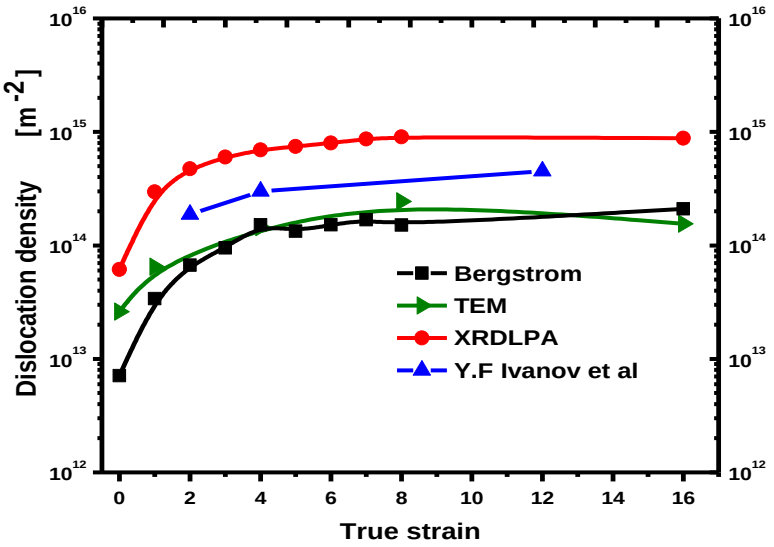

Figure 7. Dislocation densities calculated by different methods. Experimental data from Ivanov et al are also included.

In the third method, Bergström [1] established a relationship between the dislocation densities as a function of the strain (equation (2)). By using the well-known equation (3), dislocation density can be converted to stress and a stress-strain relationship can be obtained (equation (3)). Bergström considers the interaction between two types of dislocations (mobile and immobile) associated with four processes: creation, annihilation, remobilization and immobilization of dislocations [1].

$$\rho = \frac{U - A}{\Omega}(1 - e^{-\Omega\varepsilon}) + \rho_o e^{-\Omega\varepsilon} \quad (2)$$

Here U is the work hardening term, Ω is the softening term, A is a probability of remobilistaion of dislocations, and ρ_o is the initial dislocation density.

$$\sigma = \sigma_{io} + \alpha G b\sqrt{\rho} \quad (3)$$

$$\sigma = \sigma_{io} + \alpha G b\left\{\frac{U - A}{\Omega}(1 - e^{-\Omega\varepsilon}) + \rho_o e^{-\Omega\varepsilon}\right\}^{\frac{1}{2}} \quad (3)$$

According with the latter equation and taking from the literature typical values for Fe σ_{io}=60MPa; α=0.3 (a material constant); G=82GPa (shear modulus); b =2.48*10^{-10}m (Burgers vector) and assuming ρ_o=7*10^{12}m^{-2}, a fitting of the yield stress as a function of the number of ECAP passes can be carried out. The values of dislocation densities obtained in this way are shown in Figure **7** (black line).

One can see in Figure 7 that the values calculated by TEM and by the Bergström model are quite similar. However those values are different with those reported by Ivanov et al [11]. This difference, as already mentioned, can arise from the different processing conditions (route and die configuration). Another important observation is the big difference between the values calculated by XRDLPA and those obtained by TEM and Bergström model. This is because crystallite size determined by XRDLPA is often smaller than the grain or subgrain size obtained by TEM especially when the material has been processed by severe plastic deformation [15, 16]. Subgrains are separated by dipolar dislocation walls, but without differences in orientation, and this can break down coherency of X-rays scattering. Dipolar dislocation walls are one of the most common dislocation configurations in plastically deformed crystalline materials. They do not cause tilt or twist between the two delineated regions [17] therefore, it is not trivial whether they break down coherent scattering. In this way the lattice planes on the two sides of the dipolar dislocation wall will be shifted relative to each other. The shift of the lattice planes induce phase shifts in the scattered X-rays. As a result, the intensities and not the amplitudes of the scattered rays will add up, which means that there will be no coherency between the rays scattered by the different subgrains, and the line broadening will be determined by the average subgrain size. For that reason, size and size-distributions determined by XLPA better correspond to subgrains or dislocation cells [15].

Finally it is observed a saturation of the dislocation densities after five passes which could be attributed to the simultaneous occurrence of mechanisms of dislocation multiplication and

https://doi.org/10.1557/opl.2016.81

annihilation which lead eventually not only to the saturation in the grain size but also in the flow stress as shown in Figure **3**Figure **4** andFigure **6**.

CONCLUSIONS

A great reduction in the grain size with the prevalence of HAGB was obtained in Armco iron after 16 ECAP passes following route B_C at room temperature.

The strength of the material increased with the number of ECAP passes. Particularly the ultimate tensile stress reached a maximum of ~900MPa after 16 passes, which is more than three times higher as compared to that of the annealed material. Nevertheless, the tensile ductility was reduced. The increase in strength was attributed to the reduction of the grain size through refined sub-grains with high density of dislocations.

TEM method and Bergström theory calculations show similar values of dislocation densities, whereas the XRDLPA method shows higher values.

A saturation of the dislocation density was attained after four passes, which is also in good agreement with the saturation of grain size after same number of passes. This could be attributed to the simultaneous occurrence of dislocation multiplication and annihilation which leads eventually to dynamic equilibrium of the dislocation density.

ACKNOWLEDGMENTS

JAMB thanks the FPU scholarship received by the Spanish Education Ministry. Authors also thank the support of the mechanical testing service of CTM, especially Mr. Eduard Pla.

REFERENCES

[1] Y. Bergström, "A dislocation model for stress-strain behavior of polycrystalline alfa-Fe with special emphasis on the variation of the densities of mobile and immobile dislocations," *Mater. Sci. Eng,* vol. 5, pp. 193-200, 1969-1970.

[2] N. Hansen and C. Barlow, "Plastic Deformation of Metals and Alloys," in *Physical Metallurgy*, United Kingdom, Elsevier B.V., 2014, pp. 1681-1764.

[3] B. Bay, N. Hansen, D. Hughes and D. Kuhlmann-Wilsdorf, *Acta Metal Mater,* vol. 40, pp. 205-219, 1992.

[4] J. Muñoz Bolaños, O. Higuera Cobos and J. Cabrera Marrero, "Strain hardening behavior of ARMCO iron processed by ECAP," *IOP Conf. Ser.: Mater. Sci. Eng,* vol. 63, p. 012143, 2014.

[5] Y. Gang, Y. Mu-xin, L. Zheng-dong and W. Chang, *Journal of Iron and Steel Research,* vol. 18, no. 12, pp. 40-44, 2011.

[6] K.-T. Park, S. Han, B. Ahn, D. Shin, Y. Lee and K. Um, *Scripta Materialia,* vol. 51, pp. 909-913, 2004.

[7] Y. Ding, J. Jiang and A. Shan, *Materials Science and Engineering A,* vol. 509, pp. 76-80, 2009.

[8] U. Martin, U. Muhle and O. Heinrich, "The quantitative measurement of dislocation

density in the transmission electron microscope," *Parkt. Metallogr*, vol. 32, p. 467, 1995.

[9] K. Kim, J. Lee, H. Kim and Z. Lee, "Quantitative Evaluation of Dislocation Density in Epitaxial GaAs Layer on Si Using Transmission Electron Microscopy," *Applied Microscopy*, vol. 44, no. 2, pp. 74-78, 2014.

[10] L. Lutterotti, S. Matthies and H. R. Wenk, "MAUD (Material Analysis Using Diffraction): A user friendly Java program for Rietveld Texture Analysis," *Proceeding of the Twelfth International Conference on Textures of Materials (ICOTOM-12)*, p. 1599, 1999.

[11] Y. Ivanov, A. Panin, A. Son, V. Kopylov and V. Klimenov, "STRUCTURAL ANALYSIS OF ARMCO IRON SUBJECTED TO EQUAL CHANNEL ANGULAR EXTRUSION," *Russian Physics Journal*, vol. 48, no. 4, pp. 406-411, 2005.

[12] R. Valiev and T. Langdon, "Principles of Equal-channel Angular Pressing as a Processing Tool for Grain Refinement," *Progress in Materials Science*, vol. 51, pp. 881-981, 2006.

[13] Y. Zhao, H. Sheng and K. Lu, "Microstructure evolution and thermal properties in nanocrystalline Fe during mechanical attrition," *Acta Mater*, vol. 49, pp. 365-375, 2001.

[14] S. Bera, S. Chowdhury, Y. Estrin and I. Manna, "Mechanical properties of Al7075 alloy with nano-ceramic oxide dispersion synthesized by mechanical milling and consolidated by equal channel angular pressing," *Journal of Alloys and Compounds*, vol. 548, pp. 257-265, 2013.

[15] T. Ungár, E. Schafler and J. Gubicza, "Microstructure of Bulk Nanomaterials Determined by X-Ray Line-profile Analysis," in *Bulk Nanostructured Materials*, Darmstadt, WILEY-VCH, 2009, pp. 361-383.

[16] Y. T. Zhu, J. Huang, J. Gubicza, T. Ungar, Y. M. Wang, E. Ma and R. Valiev, *J. Mater. Res*, vol. 18, p. 1908, 2003.

[17] M. Wilkens, T. Ungar and H. Mughrabi, *Phys. Stat. Sol (a)*, vol. 104, p. 157, 1987.